Application Note

Zurich Instruments

Spatially resolved measurements of acid site distribution in single zeolite crystals using SRS imaging

Application: Stimulated Raman Microscopy
Products: HF2LI, UHFLI Lock-in Amplifiers

Release date: March 2015

Objectives and motivation

The development of efficient chemical processes is essential in the progress towards a sustainable economy. This greener chemistry relies heavily on efficient catalysts and, for numerous processes, heterogeneous catalysts are the most promising and sustainable candidates because of the high activity, reaction selectivity, easy separation and reusability. Optimization of catalytic materials and hence of chemical reactions necessitates gaining detailed insight into the complex physicochemical properties underlying the outcome of a catalytic process and using this information in the rational design of improved catalysts [1, 2, 3]. Acidic zeolites are widely used in the petrochemical industry as catalysts for cracking, isomerization and many other important reactions. Typically, the active sites are Brønsted acidic framework hydroxyls which are associated with the isomorphic substitution of Si(IV) by Al(III). These bridging hydroxyls line the crystalline ordered microporous network with pores typically smaller than one nanometer.

Mordenite is one of the most used zeolite catalysts in research and industry. For practical applications it has only one accessible pore system consisting of straight channels of 6.5×7.0 Å^2 that have small side pockets of 3.4×4.8 Å^2 diameter [4, 5]. For catalytic applications it is important to understand how the acid sites are distributed throughout the framework. This insight is however not easily accessible because of a lack in tools that are capable of looking beyond the crystal surface and providing relevant information with high sensitivity, high spatial resolution and chemical specificity [6, 7].

Raman microscopy offers chemical contrast as well as sub-micrometer resolution, but the interfering fluorescence background and inherently weak signals limit the application in catalyst research [8]. Amongst various signal enhancement methods developed, coherent Raman scattering microscopy is very promising due to greatly enhanced ($> 10^3$) Raman signals and universality of the technique. Coherent Anti-Stokes Raman Scattering (CARS) microscopy was first used to map the distribution of thiophene in ZSM-5 catalyst crystal [9], but the presence of non-resonant background in the CARS signal distorts the CARS spectrum and thus severely complicates the quantitative analysis [10]. The newly developed Stimulated Raman Scattering (SRS) microscopy technique, where the signal is free from non-resonant background, not only enables vibrational imaging at a speed comparable to fluorescence microscopy but also generates correct and quantitative vibrational spectra [11]. Figure 1 illustrates the basic experimental concept.

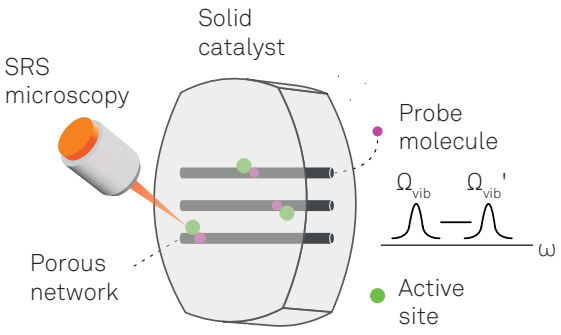

Figure 1 Schematic representation of the experimental concept. Probe molecules diffuse into the porous network and interact with the active sites, where the spectral shift in the vibrational mode of interest ($\Omega_{vib} \rightarrow \Omega_{vib'}$) reflects the properties of active sites they are attached to. Chemical mapping of the adsorbed probes at frequency $\Omega_{vib'}$ thus reveal the distribution of specific active sites in the catalyst.

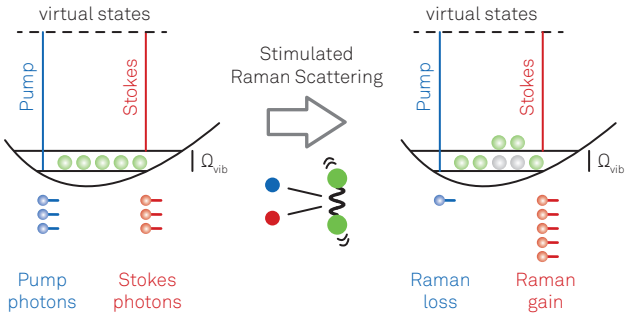

Figure 2 The schematic diagram of stimulated Raman scattering process, which results in Raman loss and Raman gain in Pump and Stokes beams, respectively.

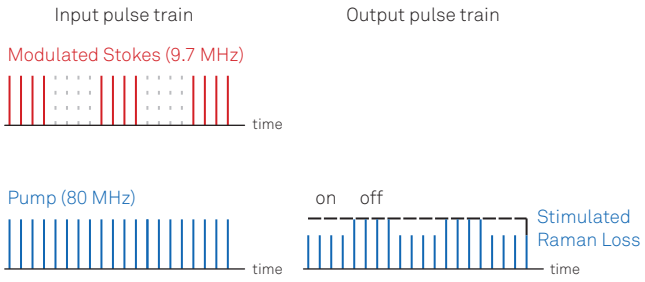

Figure 3 The lock-in amplifier detection scheme was implemented by imposing a 9.7 MHz intensity modulation on the 80 MHz pulsed Stokes beam and analyzing the modulation transfer resulting on the Pump beam (SRL) at the same frequency.

Fast imaging speeds with high resolution in 3 dimensions and straightforward spectral information are highly desired for material characterization; the short laser exposure time not only reduces the data collection time from several hours to a few minutes but also helps to avoid triggering unwanted side reaction in the catalyst during measurement. Moreover, probe molecules of different functionality for investigating various active site properties of catalysts have been documented in infrared spectroscopy literature. For example, small and large nitriles could reveal the active site distribution and accessibility, respectively [12, 13]. Hence, the combination of SRS microscopy with a deliberate choice of probes is a very powerful means to explore chemical properties of active sites hidden inside a porous catalyst. Furthermore, polarization dependence of the Raman signal unveils the orientation of probe molecules adsorbed inside the porous network; such information could help with understanding the mechanism underlying a catalytic reaction.

Recently the Roeffaers group at KU Leuven has pioneered the use of SRS microscopy with a deuterated acetonitrile probe (CD_3CN) to explore the distribution of active sites inside a single catalyst crystal. As a weak base CD_3CN can target the strong Brønsted acid framework hydroxyl sites (BAS) in H−MOR. Bulk infrared spectroscopy has shown small CD_3CN molecules effectively access all BAS in H−MOR [14, 15]. The synthetic mordenite samples used in this study contained crystals with typical crystal dimensions of 5-10 µm [16]. The H−MOR crystals were first spin-coated onto cover slip, which were then slowly calcined at 450 °C to remove possible contaminants. A few drops of liquid CD_3CN were added to the cooled-down sample. After a few hours, the treated cover slip was attached to another clear one using double-sided tape, and the sandwiched samples were ready for measurement.

Background of SRS microsocpy

In spontaneous Raman scattering, one Pump laser beam at a frequency ω_p illuminates the sample and the signal, due to inelastic scattering, is generated at the Stokes (ω_S) and anti-Stokes frequencies (ω_{AS}), respectively. The spectrum of the difference frequency between ω_p and ω_S (or ω_{AS}) reveals the vibrational energy distribution of the sample. In stimulated Raman scattering two laser beams at ω_p and ω_S must coincide on the sample. When their difference frequency, $\Delta\omega = \omega_p - \omega_S$, matches a particular molecular vibrational frequency Ω_{vib}, the Raman signal is amplified via stimulated excitation (see Figure 2).

Consequently, the intensity of the Stokes beam (I_S) experiences a gain, known as stimulated Raman gain (SRG), and the intensity of the pump beam (I_p) experiences a loss, known as stimulated Raman loss (SRL). In contrast, if $\Delta\omega$ does not match any vibrational resonance, SRL and SRG cannot occur due to the violation of energy conservation. Therefore unlike CARS, SRL and SRG do not involve the non-resonant background. Since SRL and SRG are the magnitude of intensity changes in the Pump and Stokes laser beams respectively, amplitude modulation and lock-in detection are required to record the finite SRS signal hidden in the strong background [11](see Figure 3).

In our setup, a picosecond Nd:YVO4 laser (picoTRAIN, High-Q) generating a 80 MHz pulse train at 1064 nm was employed as Stokes beam. A portion of the Stokes beam was frequency doubled to pump a temperature tuned optical parametric oscillator (Levante Emerald, APE-Berlin), whose output (700-980 nm) was then used as Pump beam.

To measure SRL signal [11], the Stokes beam was amplitude modulated at 9.7 MHz with a Pockels Cell (model 360-80, ConOptics) triggered by a function generator (Model 29, Waveteck). The Pump and Stokes pulse trains were colinearly overlapped and directed into a laser-scanning microscope (BX61WI/FV1000, Olympus), which then focused the beams onto the sample with a 25x, 1.05 NA water immersion objective (XLPLAN, Olympus). The transmitted laser beams were collected by an oil immersion condenser (U-UCD8, Olympus) and reflected out of the microscope by a dichroic mirror (FF750, Semrock), then spectrally filtered by a band-pass filter (Chroma Technology, CARS 890/220m) to remove the Stokes beam. The Pump beam was detected by a large-area silicon PIN photo-

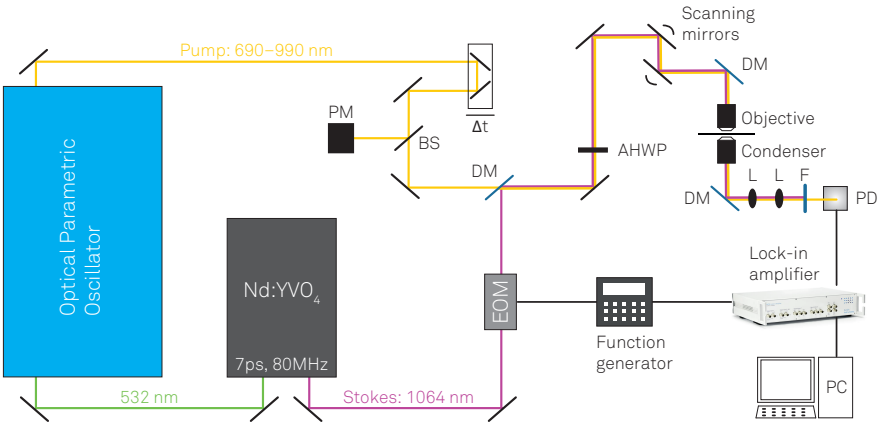

Figure 4 Schematic diagram of stimulated Raman scattering setup. AMHP: achromatic half-wave plate; BS: beam splitter; DM: dichroic mirror; EOM: electro-optical oscillator; F: filter; L: lens; PM: power meter.

diode (S8650, Hamamatsu) with a reverse bias of 60 V. The output photocurrent was band-pass filtered (Mini-Circuits, BBP-10.7+) and demodulated by a lock-in amplifier (HF2LI Lock-in Amplifier, Zurich Instruments) to retrieve the SRL signal, which was then fed into the analog-to-digital converter (FV-10-ANALOG, Olympus), synchronized with the scanning unit, to plot the chemical image. Before SRS measurement, regular white light optical transmission images of the sample were recorded with a digital camera (XC50, Olympus). Figure 4 shows the schematic of the setup.

Hyperspectral imaging was performed by sequentially tuning the OPO output with a home-built LabVIEW software and recording SRL images within a fixed field of view at each OPO wavelength, which allows us to analyze the Raman spectra in any region of interest (ROI). To normalize OPO power variation during spectral acquisition, 10% of the OPO beam was reflected with a broadband beam splitter (FS01, Semrock) and recorded by a power meter. The polarization effect in SRL signal was measured by controlling both the polarization of the pump and Stokes beams with an achromatic half-wave plate (AHWP10M, Thorlabs).

Before recording SRL images or spectra, an analyzer was used to calibrate the wave plate. With the scanning speed of todays galvo scanners one can achieve pixel dwell times of less than 10 µs which also requires a fast demodulation of the lock-in signal. The Zurich Instruments HF2LI provides a minimum time constant of 780 ns allowing for 2 µs per pixel with high SNR and sub-second SRS frame rates for images of 256×256 pixels.

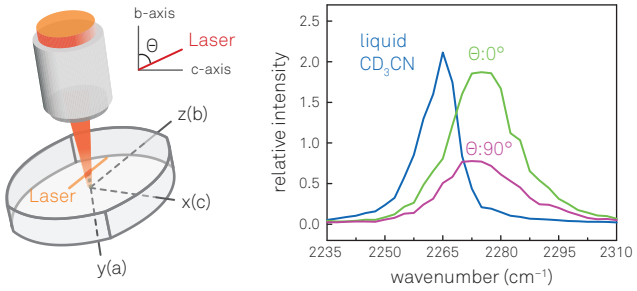

Figure 5 (Left) The schematic diagram the laser polarization with respect to crystal axis in SRS measurement. (Right) SRS spectrum of the CN stretch of liquid (×0.2) and adsorbed CD_3CN with two different orientation of laser polarization.

Measurement results

The SRS spectrum shown in Figure 5 was obtained by directly plotting the SRS intensity averaged over the whole crystal versus the Raman shift within a window of 75 cm^{-1}, which show the C ≡ N stretch of CD_3CN shifts by 10 cm^{-1}, compared to that of liquid CD_3CN, upon adsorption onto the acid site in H-MOR. In addition, the C ≡ N stretch intensity was measured for different orientations of the linear polarized excitation light with respect to the crystal axis. From detailed analysis of such polarization effects and based on theoretical calculations [17], it can be shown that CD_3CN molecules adsorbed in the main channel approach random orientation but become highly oriented along the crystallographic b-axis in the side pocket because of steric hindrance, which further implies, thanks to the linear dependence of SRS intensity on sample concentrations, about 73% of the BAS is present in the main channel and 27% is in the side pockets. These

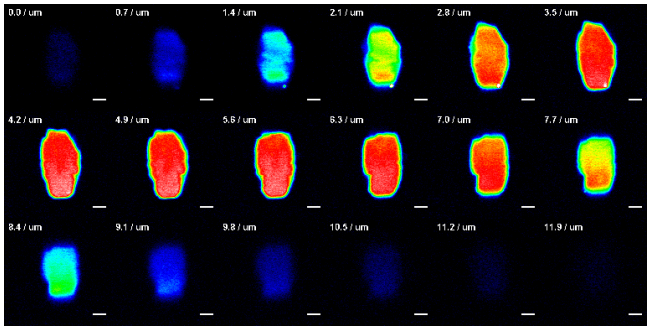

Figure 6 Montage of SRS images at the peak of CN stretch of an SP-MOR crystal at different depth. Scale bar: 3 µm.

straightforward spectral analyses on the basis of non-distorted and quantitative SRS spectra nicely highlight the advantage of SRS microscopy.
From the hyperspectral imaging scan given in Figure 6 it becomes clear that the nitrile resonance frequency throughout the whole crystal is identical and based on a homogeneous signal intensity a homogeneous distribution of BAS can be deduced. By using this information a full 3D reconstruction of the BAS inside individual MOR crystals could be done.

Summary

In summary, stimulated Raman microscopy with nitrile probe molecules allows the determination of acid site distribution at a single crystal level. This information is highly relevant to understand the catalytic performance. This approach can be applied to study the physicochemical properties of heterogeneous catalysts in general by adapting well-developed strategies in infrared spectroscopy.
A more detailed study of the acid site properties of mordenite zeolites can be found in ACS Nano, DOI: 10.1021/nn505576p

Acknowledgements

We thank Maarten B. J. Roeffaers and Kuan-Lin Liu from the Centre for Surface Chemistry and Catalysis of KU Leuven for contributing this application note.

References

[1] N. Mizuno and M. Misono, Chem. Rev., 98:199-218, 1998.

[2] K. Tanabe and W. F. Holderich, Appl. Catal. A Gen., 181:399-434, 1999.

[3] G. Busca, Chem. Rev., 107:5366-5410, 2007.

[4] P. Simoncic and T. Armbruster, Am. Mineral., 89:421-431, 2004.

[5] P. Magnoux et al., J. Catal., 106:242-250, 1987.

[6] M. B. J. Roeffaers et al., Proc. Natl. Acad. Sci. U. S. A., 104:12603-12609, 2007.

[7] T. Cordes and S. A. Blum, Nat. Chem., 5:993-999, 2013.

[8] P.-P. Knops-Gerrits et al., Microporous Mater., 8:3-17, 1997.

[9] M. H. F. Kox at al., Angew. Chem., Int. Ed., 48:8990-8994, 2009.

[10] J. P. R. Day et al., J. Phys. Chem. B, 115:7713-7725, 2011.

[11] C. W. Freudiger et al., Science, 322:1857-1861, 2008.

[12] M. Bevilacqua and G. Busca, Catal. Commun., 3:497-502, 2002.

[13] T. Barzetti at al., J. Chem. Soc. Faraday Trans., 92:1401-1407, 1996.

[14] O. Marie et al., Phys. Chem. Chem. Phys., 2:5341-5349, 2000.

[15] T. Montanari et al., Appl. Catal. A, 307:21-29, 2006.

[16] C. Hamon et al., Production of hydrocarbons from methanol in the presence of zeolite catalysts. US Pat. 4,447,669, 1984.

[17] V. D. Dominguez-Soria et al., J. Phys. Chem. C, 115:6508-6512, 2011.

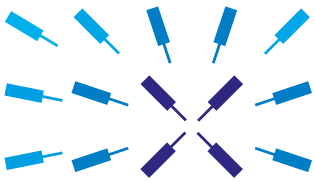

Zurich Instruments

Technoparkstrasse 1
CH-8005 Zurich
Switzerland
zhinst.com

Phone +41 44 5150 410
Fax +41 44 5150 419
Email info@zhinst.com

About Zurich Instruments
Zurich Instruments makes lock-in amplifiers, phase-locked loops, and impedance spectroscopes that have revolutionized instrumentation in the high-frequency (HF) and ultra-high-frequency (UHF) ranges by combining frequency-domain tools and time-domain tools within each product. This reduces the complexity of laboratory setups, removes sources of problems and provides new measurement approaches that support the progress of research.